Clays and Clay Minerals, Vol. 60, No. 4, 374–386, 2012.

THE DETERMINATIVE ROLE OF THE EXCHANGE CATION AND LAYER-CHARGE DENSITY OF SMECTITE ON AFLATOXIN ADSORPTION

YOUJUN DENG*, LIAN LIU, ANA LUISA BARRIENTOS VELÁZQUEZ, AND JOE B. DIXON

Department of Soil and Crop Sciences, Texas A&M University, College Section, TX 77843-2474, USA

Abstract—Using bentonites to adsorb aflatoxin is an effective method of minimizing the toxicity of aflatoxin to animals and humans. Early studies indicated a more than 10-fold difference in aflatoxin adsorption capacity among different bentonites. The determining mineralogical and chemical properties of the clays in aflatoxin adsorption are still poorly understood. The objective of this study was to test the hypothesis that a bentonite's selectivity and adsorption capacity for aflatoxin is mainly determined by the 'size matching' requirement, on a nm scale, between the non-polar interlayer surface domains and the aflatoxin molecules. The non-polar surface domain size of smectites was varied by (1) selecting smectites with different charge densities; and (2) changing the valence and the size of exchange cations to control the amount of water in the hydration shells of the cations. Infrared spectroscopy and X-ray diffraction were also used to characterize the aflatoxin-smectite complexes to investigate if layer-charge density would affect the bonding strength between aflatoxin and the minerals. A large aflatoxin adsorption capacity and high selectivity for aflatoxin were achieved by selecting smectites that had low charge density as represented by their <110 meq/100 g cation exchange capacity. An individual smectite's selectivity and adsorption capacity for aflatoxin could be enhanced or weakened by replacing the exchange cation. When the smectite was saturated with divalent cations that have smaller hydrated radius (*e.g.* Ba^{2+}), the smectite's adsorption capacity and affinity for aflatoxin were enhanced. Aflatoxin entered the interlayer of all six smectites tested. The strength of its bonding to the smectites was not affected by the layer-charge density of the smectites. The results confirmed the importance of nm-scale polarity and size match between aflatoxin molecules and the adsorbing sites on smectite. The high selectivity for aflatoxin can be achieved by selecting a smectite with adequate charge density or by replacing the exchange cations with divalent cations that have low hydration energy.

Key Words—Adsorption Capacity, Affinity, Aflatoxin B_1, Layer-charge Density, Exchange Cation, Size Matching, Smectite.

INTRODUCTION

Aflatoxins are carcinogenic metabolites produced by the fungi *Aspergillus flavus* and *A. parasitcus*. The occurrence of aflatoxins in cereal grains, oil seeds, food, and feeds is unavoidable due to heat, drought, insects, or other biological stresses during crop growth, grain transport, or storage. Since the 1970s, researchers have been testing natural and modified clay minerals as aflatoxin binders. In several studies, the clay minerals were added into animal feed and human diet as amendments to reduce the bioavailability of the toxins (Colvin *et al*., 1989; Kubena *et al*., 1990; Lindemann *et al*., 1993; Smith *et al*., 1994; Ellis *et al*., 2000; Qi *et al*., 2004; Abdel-Wahhab *et al*., 2005; Bailey *et al*., 2006; Wang *et al*., 2008; Afriyie-Gyawu *et al*., 2008a; Afriyie-Gyawu *et al*., 2008b; Phillips *et al*., 2008). The most frequently used clays in these studies are bentonites.

Bentonites are smectite-rich clays which are widely distributed around the world. Because of their important industrial and domestic applications, they are mined worldwide with an annual production of >14 million tons. Many bentonites from the USA, Japan, Mexico, India, China, and Argentina have been tested as aflatoxin binders, and they have shown varied abilities to adsorb aflatoxins *in vitro* and to reduce the bioavailability of aflatoxins *in vivo* (Masimango *et al*., 1978, 1979; Phillips *et al*., 1988; Márquez and Hernandez, 1995; Chaturvedi and Singh, 2002; Chaturvedi *et al*., 2002; Desheng *et al*., 2005; Magnoli *et al*., 2008a, 2008b).

In a continuing effort to identify the most critical mineralogical, chemical, and physical properties that affect the adsorption capacity and selectivity of bentonites for aflatoxins, numerous bentonites from different sources around the world have been evaluated. Based on these evaluations, the criteria for a 'good' natural bentonite as an aflatoxin binder were outlined as: large smectite content, small organic matter content, moderate cation exchange capacity (CEC), the presence of Fe in the octahedral sheet of the smectite, and near-neutral pH (Kannewischer *et al*., 2006; Dixon *et al*., 2008; Mulder *et al*., 2008; Tenorio *et al*., 2008). Some bentonites with large aflatoxin adsorption capacity may not have all of these properties.

Along with the successful feed and diet trials in animals and humans and the finding of more bentonites with large adsorption capacities for aflatoxins, many investigators have studied the aflatoxin–smectite reaction

* E-mail address of corresponding author:
yjd@tamu.edu
DOI: 10.1346/CCMN.2012.0600404

mechanisms at the molecular level, with the aim of understanding the scientific basis for selecting and modifying the clay minerals as an amendment for aflatoxins (Phillips *et al*., 1995, 2002; Desheng *et al*., 2005; Deng *et al*., 2010; Deng and Szczerba, 2011). The following two observations were made: (1) aflatoxin molecules could occupy the interlayer space of smectite together with exchange cations and water molecules; and (2) the infrared (FTIR) bands of adsorbed aflatoxin on smectites shifted as a function of the type of exchange cation and humidity. These observations led to speculation that the stability and selectivity of aflatoxin adsorption would be enhanced when the size and the polarity of aflatoxin molecule match those of the adsorbing nanoscale domains in the interlayer of smectite (Deng *et al*., 2010). These FTIR band shifts also led the authors to conclude that, at low humidity, the aflatoxin molecules were adsorbed to smectite through direct ion−dipole interactions and coordination between exchange cations and the carbonyl oxygens; and at high humidity, *via* H bonding between cation hydration-shell water and carbonyl groups (Deng *et al*., 2010). Quantum mechanics and molecular-dynamics simulation supported the importance of ion−dipole interactions in the bonding of aflatoxin to smectites. The computations supported the suggestion that the size of the nm-scale domains between the exchange cations in the interlayers plays a critical role in determining the selectivity of the smectite.

The objective of the present study was to test the hypothesis that smectite's high selectivity and large adsorption capacity for aflatoxins can be achieved when the size of the non-polar interlayer domains of smectite matches the size of an aflatoxin molecule. Attempts were made to achieve the optimum size of interlayer nm-scale domains by: (1) selecting six smectites with different layer-charge densities (or CECs); and (2) varying the valence and the size of exchange cations to control the density of interlayer cations and the amount of associated water in the hydration shells of exchange cations. A simplified estimation of the required size of the adsorbing domains and the charge density of the smectites was conducted first. X-ray diffraction (XRD) and FTIR spectroscopy analyses of six aflatoxin B_1-Ba-smectite complexes were conducted to check if their layer-charge density would affect the bonding strength between aflatoxin B_1 and smectites.

Theoretical consideration of the effect of charge density and exchange cation on the adsorption of aflatoxin B_1

Both computational-geometry optimization and crystal-structure measurement using XRD have revealed that an aflatoxin B_1 molecule is a co-planar configuration of the four rings, as demonstrated on the left of Figure 1 (van Soest and Peerdeman, 1970; Billes *et al*., 2006; Deng and Szczerba, 2011). When an aflatoxin B_1 molecule was projected onto a basal surface of smectite, the longest distance between two atoms in one aflatoxin molecule was ~1.5 nm (Figure 1, left) and the estimated area of the aflatoxin was 1.04 nm^2 based on the pixels of the molecule surface image. Grant and Phillips (1998) estimated the horizontal cross-sectional area of an aflatoxin molecule to be 0.883 nm^2 and the vertical cross-sectional area to be 0.528 nm^2. These estimations and the fact that the aflatoxin molecules adsorbed can tilt, rotate, vibrate, and move at their equilibration positions suggest that the actual area occupied by an AfB_1 molecule should be in the region of 0.9−1 nm^2. The basal dimensions of a montmorillonite unit cell are a = 0.518 nm and b = 0.898 nm (Viani *et al*., 2002), respectively, which give a 0.465 nm^2 basal surface area of each unit cell. This means that each aflatoxin molecule will occupy more than two unit-cell surfaces (Figure 1, left).

The specific surface area of smectite is ~800 $m^2\ g^{-1}$, or 8×10^{23} $nm^2\ kg^{-1}$. If all of the smectite interlayer surfaces were occupied by one layer of aflatoxin molecules, the estimated aflatoxin adsorption capacity would be in the range 0.66−0.78 mol kg^{-1} [*e.g.* $8 \times 10^{23}\ nm^2\ kg^{-1}/(2\ nm^2 \times 6.022 \times 10^{23})$ = 0.66 mol kg^{-1}]. This value is about half of the CEC of a smectite (100−150 meq/100 g). The largest reported aflatoxin adsorption capacity of bentonites was 0.68 mol kg^{-1} (Kannewischer *et al*., 2006).

As the basal surfaces of smectites have both polar (negatively charged) and non-polar domains, aflatoxin molecules are more likely to occupy the non-polar domains while the exchange cations would occupy the charged domains. Assuming that the average positions of interlayer exchange cations are located on a parallelogram grid (Figure 1, right) and only one layer of the adsorbed aflatoxin molecules occupy the surfaces remaining between the hydrated exchange cations, the size matching between the remaining surface area and aflatoxin would determine the maximum adsorption capacity. The unoccupied surface area among four hydrated cations on the parallelogram grid is a function of the layer charge of smectite, the valence of the cations, and the radius of the hydrated cations (Figure 2). The estimation suggested that when the interlayer space was occupied by divalent exchange cations, the remaining surface areas for other molecules were greater than when the interlayer was occupied by the monovalent cations. For example, if a smectite had a layer charge of ~0.3 per half unit cell, letting Mg, Ca, Sr, or Ba occupy the exchange sites would result in the required 1 nm^2 remaining surface area for an aflatoxin molecule. If the exchange sites of the same smectite were occupied by monovalent cations, the remaining area would only be ~0.3−0.4 nm^2. This estimation suggests that divalent cations could induce a higher selectivity of the smectite for aflatoxins.

The estimation also suggested that the size of unoccupied surface area was very sensitive to the layer-charge density of smectite. For example, to achieve the

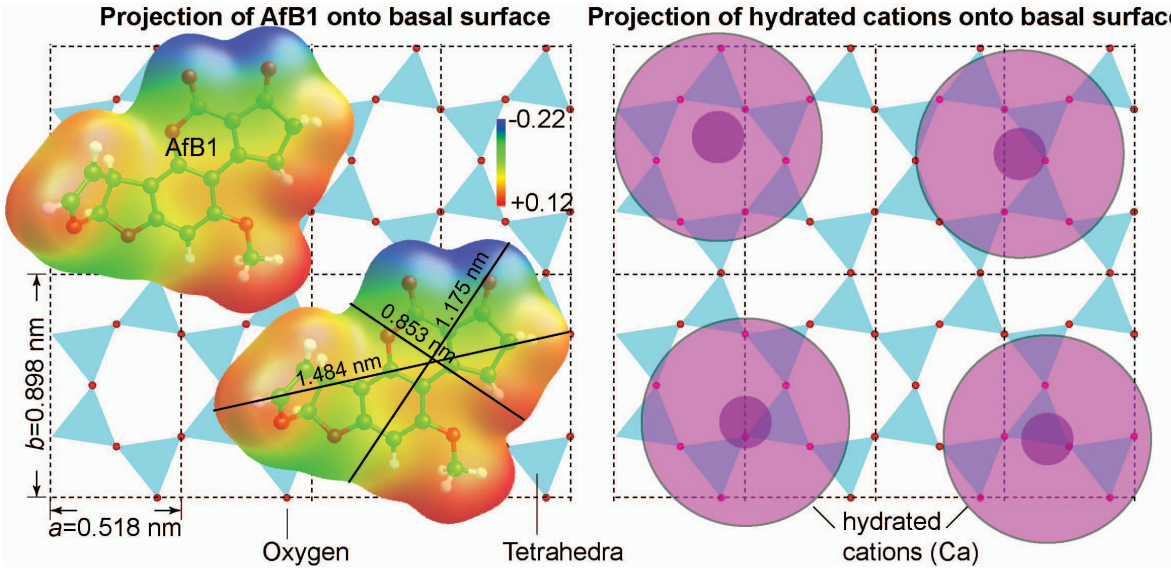

Figure 1. Conceptual models of adsorbed aflatoxin B1 molecules (left) and the hydrated exchange cations (right) projected onto the basal siloxane surfaces of 4a by 2b smectite unit cells. The color scale bar is for the surface charge of aflatoxin molecules. The smectite cell dimension is based on Viani *et al*. (2002). The aflatoxin model is reproduced with the permission of Elsevier, from Deng and Szczerba (2011).

1 nm^2 unoccupied surface area (non-polar domain), the required radius of hydrated divalent cation would be ~0.42 nm when the layer charge density was 0.3 charge per half unit cell; but the radius would have to be as small as 0.32 nm if the charge were increased to 0.35 charge per half unit cell. To verify the 'size matching' hypothesis, the effect of the smectite's layer charge density, exchanged cation valence, and the radius of the exchanged cation on the affinity and adsorption capacity of the minerals for aflatoxin B_1 was investigated.

MATERIALS AND METHODS

Smectites with different layer charges

Six bentonites were size-fractionated using sedimentation methods (Kunze and Dixon, 1986) to extract the

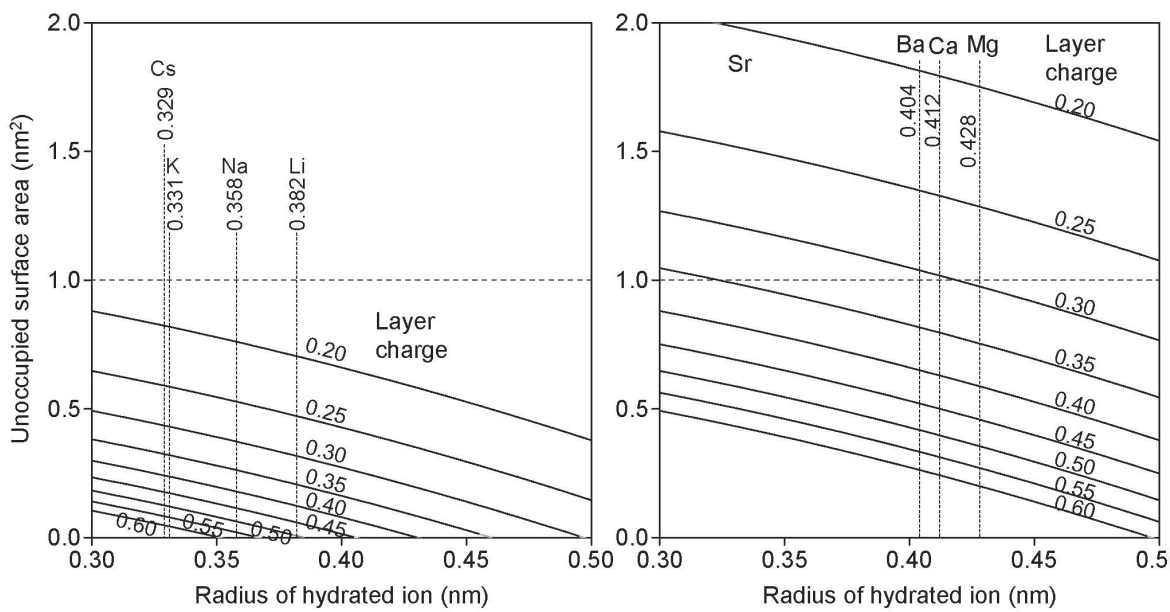

Figure 2. Unoccupied surface area remaining between hydrated cations, assuming the average positions of exchange cations are distributed on a parallelogram grid.

<2 μm smectites with different layer-charge densities (Table 1). The CEC values of the clay fractions were quantified by saturating the samples with Ca, replacing the exchanged Ca with Mg, and then measuring the concentration of exchanged Ca in solution using atomic absorption spectroscopy. The mineral compositions of the clay fractions were analyzed using XRD after saturating the clay fractions with Mg, air drying the clay dispersions to make oriented films, and solvating the air-dried films by misting a 20% (v/v) glycerol solution onto them. To evaluate their adsorption capacities for AfB_1, these samples were saturated with Ca and Ba separately. Saturation with Ca was selected because Ca is a common exchange cation in natural bentonites, and with Ba because of the enhancement of aflatoxin adsorption as demonstrated for sample 37GR. To investigate the effect of the exchange cation on aflatoxin adsorption, smectite 37GR was saturated with four monovalent cations Li, Na, K, and Cs as well as four divalent cations Mg, Ca, Sr, and Ba, respectively. For different cation saturation, 50 mg of each clay fraction were mixed with 15 mL of one of the 1 M LiCl, NaCl, KCl, or CsCl, or 0.5 M $MgCl_2$, $CaCl_2$, $SrCl_2$, or $BaCl_2$ solutions in a 50 mL centrifuge tube, shaken for 2 h, centrifuged, and then treated once more with the same electrolyte solution to ensure cation saturation. The excess electrolyte in the suspension was removed by two bouts of water washing. The resulting clay mineral dispersions were kept in a refrigerator.

Aflatoxin adsorption isotherms and their fitting

The procedures of Grant and Phillips (1998) and Kannewischer *et al*. (2006) were followed to conduct aflatoxin adsorption isotherms. In most cases, the adsorption isotherms could be fitted with the standard Langmuir equation but, in some cases, the Langmuir fitting was very poor and, therefore, an exponential Langmuir and a modified Langmuir equation with *q*-dependent affinity (QKLM) (Gu *et al*., 1994; Grant *et al*., 1998) were also used to fit the adsorption data. These equations were:

(1) Langmuir equation

$$q = Q_{\max}\left(\frac{\mathrm{K}C}{1+\mathrm{K}C}\right) \quad (1)$$

(2) exponential Langmuir equation

$$q = Q_{\max}\left(\frac{\mathrm{K}C^n}{1+\mathrm{K}C^n}\right) \quad (2)$$

(3) modified Langmuir equation with *q*-dependent affinity (QKLM)

$$q = Q_{\max}\left[\frac{\mathrm{K}e^{(-2bq)}C}{1+\mathrm{K}e^{(-2bq)}C}\right] \quad (3)$$

where q is the amount of aflatoxin adsorbed on the clay; $Q_{\max}$, the maximum adsorption capacity; C, the equilibrium concentration of aflatoxin in solution; K, the Langmuir equilibrium constant (distribution constant), which reflects the affinity of the clay mineral surface for aflatoxin which increases with the binding energy; n, an exponential parameter meaning that n types of adsorption sites are present on or in the smectite; and b, an energy-dependent affinity parameter. Non-linear least-square regression was used to refine the parameters *K,* $Q_{\max}$, n, and b with the add-in program *Solver* in Microsoft Excel ® and program *R* by minimizing the sum of squares of differences (*SSD*) between the measured and the equation-fitted adsorption values:

$$SSD = \sum_i [q(i) - q_c(i)]^2 \quad (4)$$

where $q(i)$ is the measured ith adsorption and $q_c(i)$ is the equation-fitted ith adsorption based on the Langmuir or modified Langmuir equations. The goodness-of-fit, η^2, was computed according to Schulthess and Dey (1996),

$$\eta^2 = 1 - \frac{\sum_i [q(i) - q_c(i)]^2}{\sum_i [q(i) - q_{\mathrm{mean}}]^2} \quad (5)$$

which is similar to the commonly used *R*-square (R^2) of a linear correlation equation. The standard errors of the

Table 1. Mineralogy and chemical properties of the clay-size fractions of the six bentonites tested.

Sample	Origin	Clay mineral content in bulk (g/kg)[a]	Non-smectite minerals	CEC[b] (meq/100 g)	Estimated smectite layer charge (charge/half unit cell)[d]
7AZ	Arizona, USA	847	N.D.[c]	138.4	0.50
5OK	Oklahoma, USA	767	N.D.	136.6	0.49
37GR	Greece	757	N.D.	111.5	0.40
1MS	Mississippi, USA	670	N.D.	107.7	0.39
8TX	Texas, USA	839	Halloysite (trace)	94.6	0.34
16MX	Mexico	559	Kaolinite, feldspar	78.1	?

[a]: based on size fractionation; [b]CEC: cation exchange capacity; [c]N.D.: none detected; [d]Assuming the specific basal surface area of smectite is 780 m^2 and each unit cell has a basal surface area of 0.465 nm^2.

parameters Q_{max}, K, n, and b were estimated using program *R*. In most cases, programs *R* and *Solver* yielded the same estimated values for the parameters. In a few cases where the adsorption isotherms were too far away from the L shape, the estimated values from program *R* yielded poorer fitting and, therefore, the parameters estimated by *Solver* were reported here but the standard errors of these values were not calculated.

Synthesis and analysis of aflatoxin B_1-Ba-smectite complexes

The adsorption experiment indicated that the Ba-saturation induced high aflatoxin adsorption for all of the six smectites. To form AfB_1-Ba-smectite complexes for FTIR spectroscopy and XRD characterization, 1 mg of each of the six Ba-saturated clays was mixed with 35 mL of 8 ppm AfB_1 solution, shaken for 24 h at 200 rpm on a rotary shaker and centrifuged, the supernatant was replaced by another 30 mL of fresh 8 ppm AfB_1 solution, and then the treatment was repeated once more. After each centrifugation, the supernatant was collected to quantify AfB_1 concentration. After the two AfB_1 treatments, the resulting AfB_1-Ba-smectite complexes were washed three times with deionized water to remove excess AfB_1. The washed complexes were kept in ~0.5 mL deionized water as suspensions and stored at 4ºC.

Fourier-transform infrared spectroscopy

Each aflatoxin-B_1-Ba-smectite complex suspension was air dried on a 25 mm × 2 mm ZnS disc (ClearTran, International Crystal Labs, Garfield, New Jersey, USA) and mounted in a dewar accessory (model DER-P11-3, Harrick Scientific Products, Inc. Pleasantville, New York, USA). To reach nearly 100% humidity, a piece of wet Kimwipe tissue was placed in the sample chamber of the dewar; to reach nearly 0% humidity, the chamber was purged with dry N_2 gas. The spectra were recorded on a Spectrum 100 Fourier-transform infrared spectrometer (Perkin-Elmer). After the FTIR spectroscopy analysis, each complex was washed off the ZnS disc and re-dispersed in water for XRD analysis.

Variable-temperature XRD

The re-dispersed complex suspension was air dried on the polished side of a 0.50 mm × 130 mm × 150 mm silicon plate cut from a (100) silicon wafer (University Wafers, Boston, Massachusetts, USA). The plate was placed on top of the sample cup of a reactor chamber XRK 900 (Anton Paar Gmbh, Graz, Austria) and carefully aligned with respect to the goniometer axis of a Bruker D8 Advance X-ray diffractometer. The (400) diffraction peak of silicon (69.132º2θ for CuKα_1 radiation) was used to calibrate and to adjust the sample-stage height. The sample was heated at a rate of 0.1ºC/s and was maintained at the desired temperature when XRD patterns were recorded. The diffractometer (CuKα radiation) was operated at 35 kV and 45 mA with a step size of 0.05º2θ and a dwell time of 3 s per step. An energy dispersive detector Sol-X was used for the analysis. Programmable divergence and anti-scattering slits were set to v12 (12 mm irradiation length). The XRD patterns of one Ba-smectite (37GR) at elevated temperatures were also recorded to monitor the collapse of smectite under the same heating scheme.

RESULTS

Mineralogy of the clay fractions

As indicated by the intense 1.8 nm peaks on the XRD patterns (Figure 3), smectites were the dominant or only mineral in the clay fractions of the six bentonites. No other crystalline phases were found in samples 1MS, 5OK, 7AZ, or 37GR by XRD or scanning electron microscopy (SEM) (data not shown), a trace amount of halloysite was observed in sample 8TX under SEM but it was not detectable by XRD, confirming its small abundance. Appreciable amounts of kaolinite and albite were detected in sample 16MX (Figure 3). No opal-C or opal-CT was detected in these samples. Due to the simple mineral compositions of samples 1MS, 5OK, 7AZ, 8TX, and 37GR, all of the CEC values of the clay fractions were attributed to smectites and were used to estimate the layer charge of the smectite in each sample (Table 1), assuming the smectites had a specific basal surface area of 780 $m^2\ g^{-1}$ and that each unit cell had a basal surface area of 0.465 nm^2 (a = 0.518 nm and b = 0.898 nm, Viani *et al*., 2002). Samples 5OK and 7AZ were noted to have much larger CEC and charge-density values than the other samples. Due to the presence of kaolinite and feldspars in sample 16MX, the layer charge of smectite could not be estimated unambiguously.

Effects of exchange cation and charge density on aflatoxin adsorption

The valence and size of the exchange cation and the layer-charge density significantly affected the affinity and adsorption capacity of smectite for aflatoxin B_1. The adsorption isotherm shape also changed with the exchange cation and charge density. Not all of the adsorption isotherms could be fitted well with the standard Langmuir equation. The adsorption isotherms were of either S-, C-, or L-type, suggesting different affinities of the surfaces and different adsorption mechanisms.

Effect of exchange cation on aflatoxin adsorption

In general, experimentally observed changes in aflatoxin B_1 adsorption on 37GR due to exchange cations were in agreement with the trends predicted from the estimation based on Figure 1. The monovalent cation-saturated 37GR showed lower affinity for aflatoxin than the divalent cation-saturated 37GR (Table 2, Figure 6). For both monovalent and divalent cation saturations, decreasing the radius of the hydrated cation

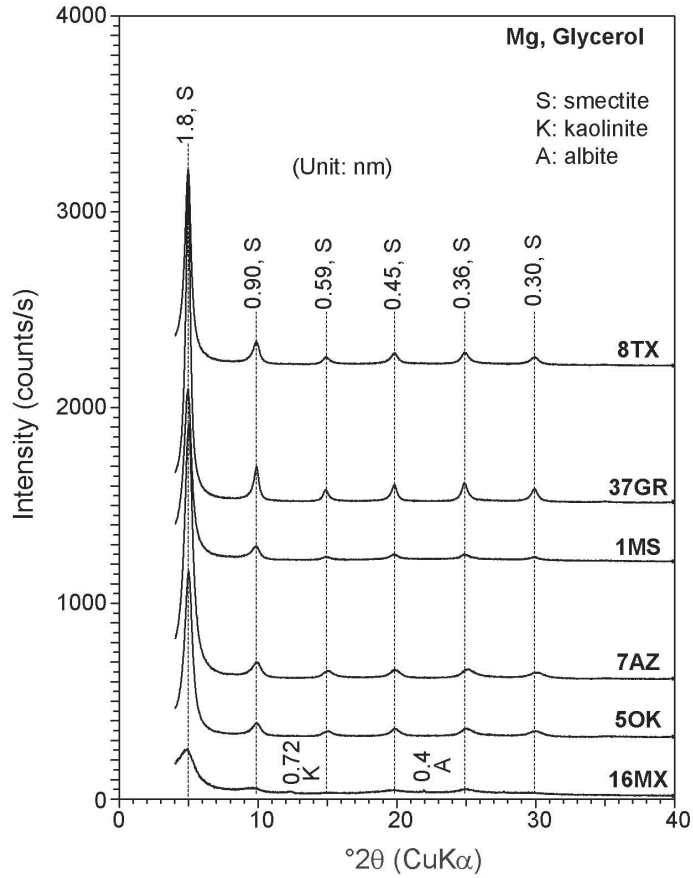

Figure 3. XRD patterns of oriented <2 μm clay fractions saturated with Mg and solvated with glycerol.

appeared to increase the smectite's affinity, adsorption capacity, or both, for aflatoxin B_1. The greatest affinity and adsorption capacity were observed for Ba-saturated 37GR and the lowest affinity and adsorption capacity were observed for Li-saturated 37GR. Exceptions from the general trends were observed for Cs and Sr. In addition to reducing the affinity and adsorption capacity for aflatoxin, exchange cations Li and Na also altered the adsorption isotherms to the C-type and S-type shapes, and the standard Langmuir fitting resulted in unrealistic Q_{max} and K values (Table 2).

The general trends observed among the exchange cations and the exceptions displayed for Cs and Sr indicated that affinity and adsorption capacity for aflatoxin by a particular cation-saturated smectite are the compromised results of size matching and the bonding strength. The hydrated Cs has a similar radius (0.329 nm) to a hydrated K (0.331 nm), but the radius of a dehydrated Cs (0.186 nm) is much greater than that of a dehydrated K (0.149 nm). The similar sizes of hydrated Cs and K suggest that they do not alter the unoccupied surface areas by means of hydrated cations, but the larger size of the dehydrated Cs would induce a much weaker ion−dipole interaction between the cation and the oxygen on aflatoxin molecules. The ion−dipole interaction between the exchange cation and the carbonyl oxygen on aflatoxin is one of the major bonding mechanisms for the adsorption of aflatoxin in both dehydrated and hydrated smectite (Deng *et al*., 2010; Deng and Szczerba, 2011).

Effect of smectite layer charge on the adsorption of aflatoxin

The six smectite samples with Ca or Ba saturations showed substantial differences in affinity and adsorption capacity for AfB_1. Depending on the adsorption isotherm fitting models, the six clays had up to a three-fold difference in adsorption capacity (Q_{max}) and as much as a hundreds-fold difference in affinity (constant K) (Table 2, Figures 4−6). Samples 1MS, 8TX, and 37GR had large adsorption capacity and affinity values, and their aflatoxin adsorption isotherms could be fitted well with the standard Langmuir model (Table 2). Samples 5OK and 7AZ showed S-type adsorption isotherms, which suggested their low affinity for aflatoxins when the aflatoxin concentration was low. In other words, aflatoxin molecules had to overcome a high energy barrier to stay at the surfaces or diffuse into the interlayer of the minerals. The adsorption isotherms of sample 5OK and 7AZ could only be fitted well with the

Table 2. Adsorption isotherm fit parameters for aflatoxin adsorption on the clay-mineral samples saturated with different cations*.

Sample	Exchange cation	Langmuir			Exponential Langmuir				Modified Langmuir QKLM			
		Q_{max} (mol kg^{-1})	K ((μM)$^{-1}$)	η^2	Q_{max} (mol kg^{-1})	K	*N*	n^2	Q_{max} (mol kg^{-1})	K	*b*	η^2
37GR	Li	0.497±0.388	0.018±0.019	0.889	0.202±0.092	0.0105±0.015	1.75±0.87	0.900	0.198±0.057	0.021±0.005	6.39±4.14	0.974
	Na	27.3**	0.0004**	0.978	5.802**	0.001**	1.215**	0.988	0.383±0.079	0.0176±0.002	−2.97±0.90	0.996
	K	0.632±0.023	0.129±0.011	0.995	0.668±0.078	0.128±0.012	0.946±0.097	0.995	0.593±0.057	0.127±0.012	−0.27±0.42	0.995
	Cs	0.378±0.038	0.088±0.020	0.972	11.6**	0.004**	0.525**	0.986	0.356±0.124	0.088±0.020	−0.36±2.13	0.972
	Mg	0.516±0.021	0.280±0.038	0.983	0.505±0.046	0.280±0.040	1.04±0.17	0.983	0.478±0.029	0.224±0.054	−0.81±0.68	0.986
	Ca	0.595±0.034	0.351±0.064	0.968	0.509±0.024	0.322±0.049	1.53±0.21	0.984	0.517±0.021	0.201±0.044	−1.61±0.52	0.989
	Sr	0.713±0.055	0.143±0.027	0.975	0.550±0.033	0.110±0.022	1.53±0.20	0.989	0.549±0.022	0.096±0.014	−1.64±0.38	0.994
	Ba	0.718±0.029	0.395±0.049	0.985	0.638±0.029	0.423±0.042	1.288±0.134	0.991	0.634±0.021	0.275±0.040	−0.99±0.29	0.994
1MS	Ca	0.636±0.015	0.448±0.041	0.993	0.632±0.033	0.450±0.046	1.012±0.099	0.993	0.629±0.030	0.435±0.071	−0.09±0.36	0.993
	Ba	0.692±0.017	0.826±0.093	0.990	0.700±0.036	0.804±0.119	0.971±0.108	0.990	0.693±0.030	0.832±0.173	0.02±0.37	0.990
8TX	Ca	0.627±0.021	0.547±0.074	0.982	0.600±0.033	0.577±0.084	1.12±0.15	0.984	0.589±0.026	0.423±0.104	−0.70±0.50	0.986
	Ba	0.662±0.022	0.868±0.123	0.978	0.618±0.022	1.038±0.159	1.29±0.17	0.984	0.619±0.017	0.536±0.124	−1.06±0.41	0.989
7AZ	Ca	1.09±0.57	0.009±0.006	0.985	0.256±0.020	0.008±0.002	1.85±0.16	0.997	0.237±0.009	0.025±0.001	−4.89±0.48	0.999
	Ba	0.983±0.207	0.033±0.010	0.981	0.451±0.024	0.022±0.004	1.79±0.14	0.997	0.440±0.023	0.040±0.004	−2.52±0.45	0.996
5OK	Ca	27.1**	0.0004**	0.955	0.239±0.012	0.0008±0.0005	2.89±0.27	0.996	0.237±0.012	0.017±0.003	−6.92±1.01	0.996
	Ba	0.840±0.215	0.044±0.018	0.953	0.386±0.010	0.008±0.002	2.61±0.19	0.996	0.405±0.098	0.034±0.004	−3.59±0.33	0.998
16MX	Ca	0.246±0.013	0.109±0.014	0.988	0.220±0.022	0.103±0.016	1.149±0.157	0.990	0.213±0.019	0.0970±0.017	−1.93±1.49	0.991
	Ba	0.308±0.017	0.138±0.021	0.982	0.276±0.028	0.133±0.024	1.166±0.187	0.984	0.268±0.023	0.117±0.028	−1.71±1.41	0.986

* Parameters Q_{max}, *K, n*, and *b* are reported as "estimated value ± standard error." The model parameters were estimated using program *Solver* in MS Excel® and program *R*, whereas the standard errors were estimated with program *R*. In most cases, programs *R* and *Solver* yielded the same estimated values for the parameters.

**In a few cases, whereas the adsorption data points were too far away from the L-shape, program *R* yielded much poorer fitting curves than *Solver* and, therefore, the parameters estimated by *Solver* were reported here but the standard errors were not calculated.

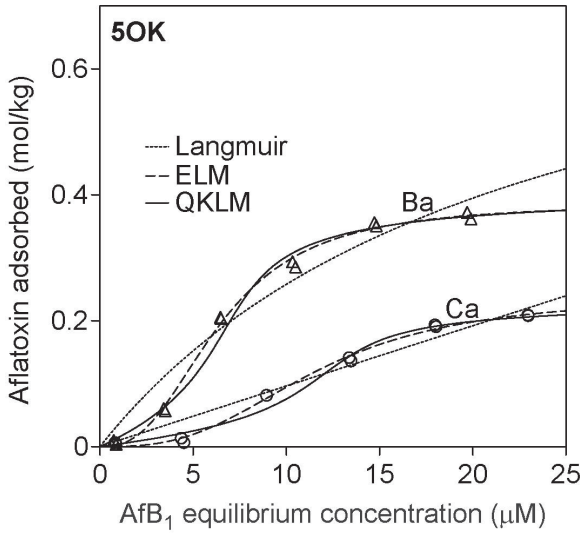

Figure 4. Langmuir, exponential Langmuir (ELM), and modified Langmuir (QKLM) fits of aflatoxin adsorption isotherms on Ca- and Ba-saturated smectite extracted from bentonite 5OK.

exponential Langmuir model or the modified QKLM model (Table 2, Figure 4). By comparing the adsorption capacity and affinity with the charge properties of the samples (Table 1), smectites with CEC values between 94 and 112 meq/100 g, or a charge density between 0.34 and 0.40 charge per half cell, were the best for adsorption of aflatoxin.

On all of the six smectite samples tested, saturation with Ba resulted in greater aflatoxin adsorption than Ca saturation. The largest increase, almost double the original, was observed for the high-charge-density smectites 5OK and 7AZ. The increase in aflatoxin adsorption suggests greater sensitivity of the high layer-charge smectites to the exchange cation.

Sample 16MX had a CEC of 78.1 meq/100 g, due partly to a dilution effect of kaolinite and feldspars. If the smectite in this clay had the same CEC as the 1MS or 8TX, 16MX would be expected to have ~80% of the adsorption capacity of the two latter samples. Yet only ~40% of their adsorption capacity was observed on this clay and the difference between Ca and Ba saturations was small. The poor adsorption of aflatoxin on this sample and the milder response to the type of exchange cation deserve more study.

Characterization of the AfB_1-Ba-smectite complexes

During the synthesis of AfB_1-Ba-smectite complexes, the majority (>80%) of the aflatoxin adsorption occurred in the first treatment of smectites with AfB_1 solution (Table 3). The significant reduction of AfB_1 adsorption in the second treatment suggested that smectites were saturated or nearly saturated with AfB_1 after the two treatments.

The *d* spacings of the smectites, *e.g.* 37GR shown in Figure 7, collapsed to 1.0 nm when heated to >150ºC, but for the AfB_1-Ba-smectite complexes the *d* spacing value was always greater than the smectites with values of between 1.25 and 1.45 nm at 300ºC. The greater *d* spacings of the complexes at elevated temperatures suggested that aflatoxin B_1 molecules went into the interlayers of all six smectites. The XRD analysis also indicated that the d_{001} spacings of the complexes, except sample 16MX, were roughly proportional to the AfB_1 loadings in the complexes (Table 3). Samples 8TX and 1MS had the greatest AfB_1 loadings and also had the largest d_{001} spacing of 1.6 nm at 30ºC. Samples 5OK and 7AZ had the smallest *d* spacings of 1.36−1.40 nm (Figure 7). The trend of larger *d* spacings associated with greater AfB_1 loadings remained at elevated temperatures. The AfB_1-Ba-smectite complex of 16MX had *d* spacings between those of 37GR and 7AZ during the heating, but had the smallest AfB_1 loading. Again, the lower AfB_1 loading was due to the dilution effect of kaolinite and feldspars in the sample.

Except for the difference in FTIR band intensity due to different loadings of AfB_1 in the six AfB_1-Ba-smectite complexes, the FTIR bands of adsorbed AfB_1 in the six complexes showed essentially the same positions, shape, broadness, and shifts with humidity (Figure 8). The detailed FTIR band assignments were discussed by Deng *et al.* (2010) and only a few of the major bands are discussed here. The identical band positions and shifts of the six complexes suggested that the AfB_1 was bonded to the smectites with the same mechanisms of direct ion−dipole interactions between the exchange cation and the oxygen (predominantly the two carbonyl oxygen atoms) of the AfB_1, as well as the H bonding between the hydration shell water of the exchange cation and the oxygen atoms of the AfB_1 (Deng *et al*., 2010; Deng and Szczerba, 2011). When recorded at 0% humidity, the FTIR band positions of adsorbed AfB_1 in the six AfB_1-Ba-smectite complexes were very close to those of an AfB_1-Ca-smectite reported by Deng *et al.* (2010). For example, the in-phase stretching vibrations of the two carbonyl groups in the AfB_1-Ba-smectite complexes occurred at 1725 cm^{-1} (Figure 8), whereas they occurred at 1727 cm^{-1} in the AfB_1-Ca-smectite complex. According to Billes *et al*. (2006) the opposite-phase stretching (1635 cm^{-1}) and the bending vibrations (1590 cm^{-1}) of the two C=O bonds in AfB_1-Ba-smectite complexes differed by no more than 2 cm^{-1} from those of the AfB_1-Ca-smectite complex. The nearly identical FTIR

Table 3. Quantities of aflatoxin loaded (mol kg^{-1}) during synthesis of AfB_1-Ba-smectite complexes.

AfB_1 treatment	1MS	5OK	7AZ	8TX	16MX	37GR
1st	0.61	0.35	0.40	0.56	0.22	0.60
2nd	0.12	0.08	0.08	0.08	0.02	0.08
Total	0.73	0.43	0.49	0.65	0.25	0.68

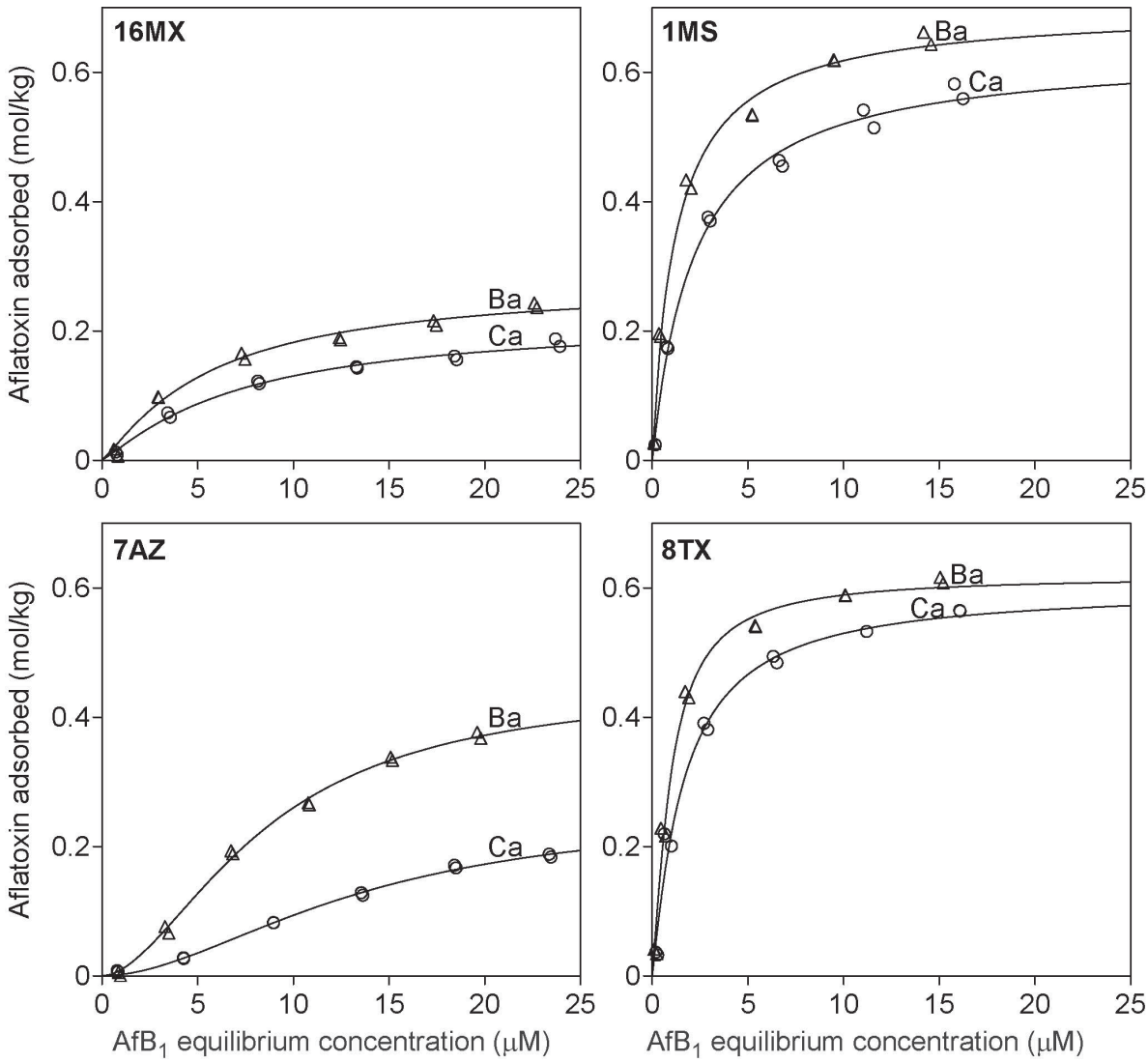

Figure 5. Aflatoxin adsorption isotherms on Ca- and Ba-saturated smectites extracted from bentonite 1MS, 7AZ, 8TX, and 16MX. The curves are the exponential Langmuir fits.

band positions suggested that the Ba and Ca saturations of smectites induced about the same bonding strength between the AfB_1 molecules and smectites. The layer-charge density difference among the six smectites caused no detectable differences in the FTIR band positions and, therefore, the bonding strength.

DISCUSSION

Overall, the effects of the charge density of smectite and the type of exchange cation on aflatoxin adsorption were in agreement with the ''size matching effects'' observed in the adsorption of many cationic and non-ionic organic compounds on smectites (Takahashi-Ando *et al*., 2002; Takagi *et al*., 2010; Egawa *et al*., 2011; Laird *et al*., 1992; Sheng *et al*., 2002; Liu *et al*., 2012). Yet, the specific influence of the type of exchange cation on the adsorption of aflatoxin differed considerably from other smaller organic compounds.

The size-matching effect on cationic compounds is easy to understand as the distances between cationic sites in an organic compound must match the distance from the negative-charge sites of smectite layers. This requirement has guided the design of several novel porphyrin derivative-saponite complexes to vary the absorption peak positions and excited lifetimes of the dyes, to harvest light, and to transfer energy in the complexes (Ishida *et al*., 2012). These properties are attractive for constructing efficient photochemical reaction systems (Takagi *et al*., 2006, 2011). Dealing with the adsorption of non-ionic compounds by smectites is less straightforward as they were not adsorbed by means of cation-exchange reactions and no charge-balance requirement was involved. Several studies have reported

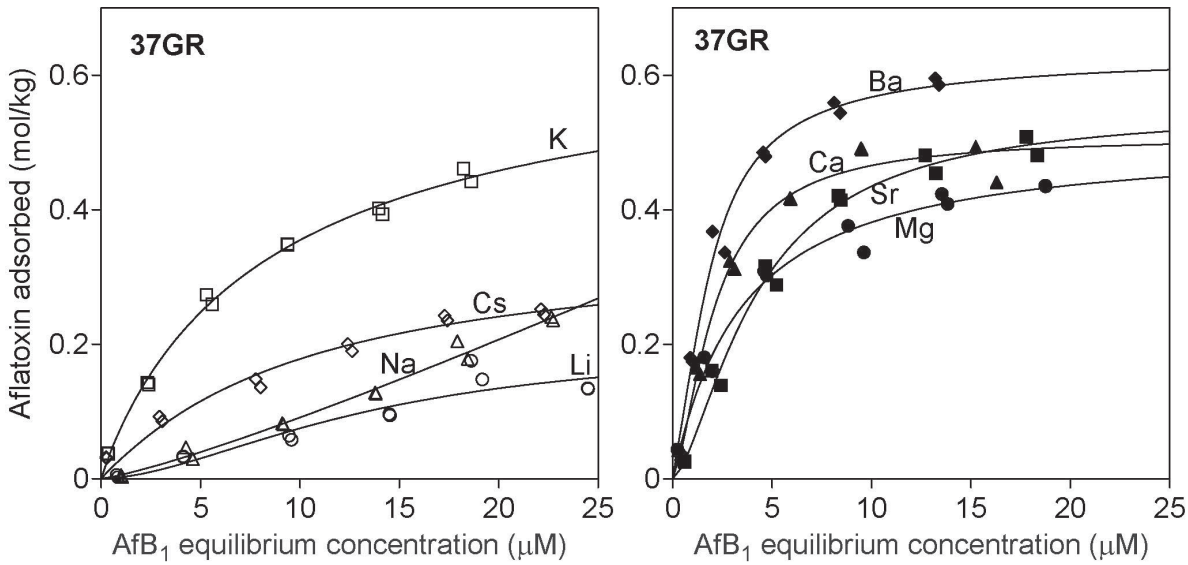

Figure 6. Aflatoxin adsorption isotherms on Li-, Na-, K-, Cs-, Mg-, Ca-, Sr-, and Ba-saturated smectites extracted from bentonite 37GR. The curves are the exponential Langmuir fits.

inverse relationships between the adsorption affinity of nitroaromatic compounds, atrazine, and dioxane with the CEC or the charge density of smectites (Laird *et al*., 1992; Pereira *et al*., 2008; Su and Shen, 2009; Liu *et al*., 2012). In the study of adsorption of dinitrophenol herbicides, 2,4-dinitro-o-cresol and 4,6-dinitro-o-sec-butyl phenol, Sheng *et al*. (2002) found that, under their experimental conditions, the herbicides were adsorbed mainly as neutral species. They found that the adsorption capacity of montmorillonites (natural or modified by reducing the CEC with the Hofmann-Klemen effect) for the herbicides was inversely correlated to the CEC of the clays and attributed the greater adsorption of the lower charge-density montmorillonite to their larger adsorption domain size. Sheng *et al*. (2002) observed that K- or Cs-saturation of a montmorillonite resulted in a much more effective clay for adsorbing the herbicides than the Al-, Na-, Ba-, or Ca-saturation of the same clay and suggested that this effect was due to the smaller size of the hydrated K and Cs, which allow for a larger adsorbing domain size for the pesticides and also might have induced the optimal *d* spacing of ~1.25 nm for the monolayer adsorption of the herbicides.

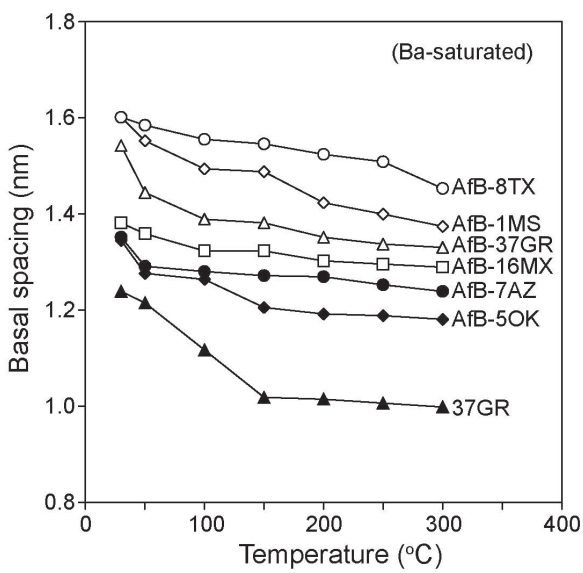

Figure 7. Basal spacing of Ba-37GR and Ba-saturated aflatoxin B1-smectite complexes at elevated temperatures.

Atrazine is a weak basic herbicide but was adsorbed primarily as a neutral species by smectites (Laird *et al*., 1992). Its adsorption on smectites was also inversely related to the charge density of the smectites. The siloxane surfaces with lower charge densities had greater affinities for atrazine than those with higher charge densities (Laird *et al*., 1992). Rather like the findings on the adsorption of dinitrophenol herbicides, Liu *et al*. (2012) observed that the adsorption of polychlorinated dibenzo-p-dioxins was inversely correlated to the charge density of the smectites and the monovalent cation Cs saturation of the montmorillonite resulted in much greater adsorption affinity of the clay for the dioxin.

Saturation of the smectite with divalent cations such as Ca and Ba resulted in much less adsorption of dioxin and the nitroaromatic compounds (Sheng *et al*., 2002; Liu *et al*., 2012). This observation differed from the adsorption of aflatoxin observed in the current study. The differences are probably due to the size of the organic compounds studied. The dioxins and the nitroaromatic compounds in their studies had molecular weights of ~200 g mol^{-1} or less, which were substantially smaller than that of aflatoxin B_1 (312 g mol^{-1}).

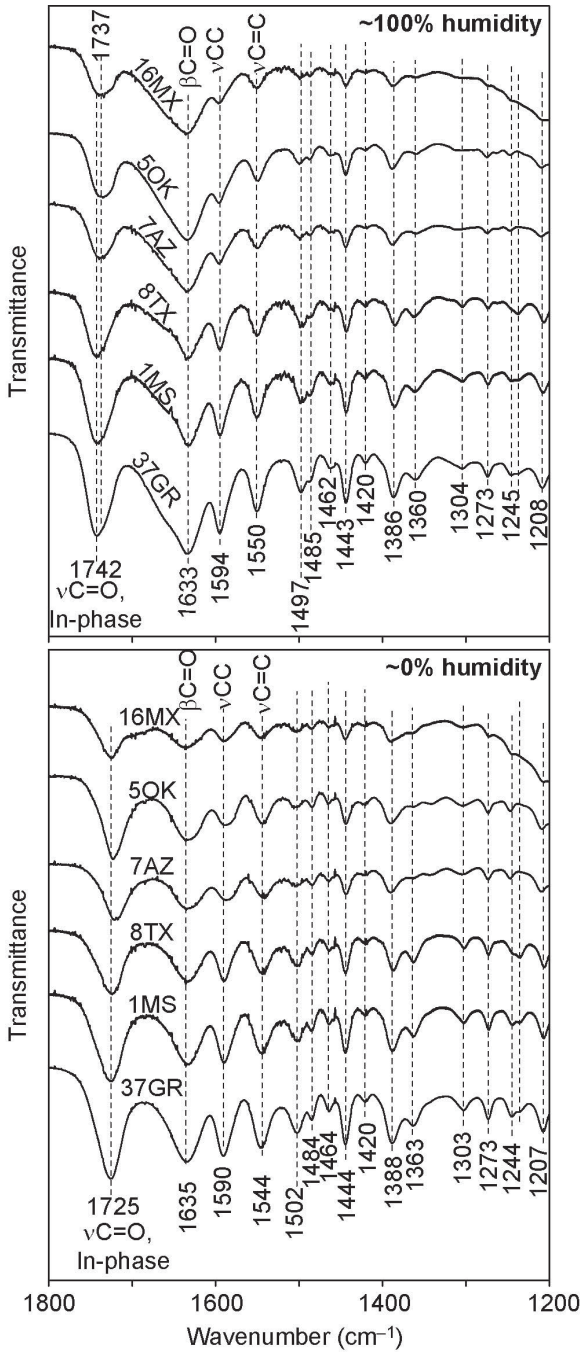

Figure 8. FTIR spectra of aflatoxin B1-smectite complexes saturated with Ba recorded at 0% and 100% humidities. Only major bands involved in aflatoxin–cation dipole interaction or H bonding were marked.

They would require a smaller surface area; and, therefore, a more crowded exchange cation environment may have a better 'size-match effect' than the divalent cation saturations.

In the study of dioxin by smectites, Liu *et al*. (2012) found that, in addition to layer-charge density, the layer-charge source and distribution also had profound effects on the adsorption capacity of the smectites. For example, among three smectites (saponite, hectorite, and montmorillonite) that had similar CECs in the range 78–86 meq/100 g, the saponite, in which nearly 100% of the layer charge originated within the tetrahedral sheets, adsorbed the largest amount of dioxin. Liu *et al*. (2012) attributed this effect to the greater proportion of the hydrophobic siloxane surfaces. Those authors estimated that only ~9% of the siloxane surface in saponite was impacted directly by the isomorphic substitution of Al for Si in the tetrahedral sheet and was, therefore, hydrophilic; the remainder was hydrophobic. A much larger and more diffuse siloxane surface portion was impacted by the more distant isomorphic substitution of Mg for Al in the octahedral sheet in montmorillonite. Liu *et al.* (2012) further stated that water was held more forcefully on the hydrophilic surface of montmorillonite and this tightly held water made the surface more difficult to access by dioxin. Whether such a layer-charge origin effect exists on the adsorption of aflatoxin is unclear. This issue and the effect of the charge source on aflatoxin bonding strength will be addressed in ongoing research.

CONCLUSIONS

The results confirmed the determinative roles of layer-charge density and the type of exchange cations in the adsorption by the smectites of aflatoxin B_1. The inverse relationship of adsorption capacity and affinity with the charge density of the smectites was in agreement with the findings made for nitroaromatic compounds, dioxin, and atrazine reported in the literature. Yet, the types of the exchange cations exerted different effects on the adsorption of aflatoxin from the effect on the adsorption of smaller organic compounds. In general, divalent cations with smaller hydration energies resulted in greater affinity and adsorption capacity of the smectites for aflatoxin, regardless of the charge density of the minerals. All smectites were capable of adsorbing aflatoxin molecules into their interlayer, but with varied saturation extents. The charge density differences among the smectites apparently had no effect on the bonding strength between aflatoxin and the smectites, which were mainly ion–dipole interaction between exchange cation and aflatoxin and the H-bonding between aflatoxin and water in the hydration shell of the exchange cations. This finding corroborated early observations that Ca-bentonites were in general better aflatoxin binders than Na-bentonites, and can be used to guide the selection and modification of bentonites for aflatoxin detoxification.

ACKNOWLEDGMENTS

Funding was supplied by Texas AgriLife Research Bioenergy Initiative Program, Texas Corn Producers

Board, National Corn Growers Association, and CONACYT-Texas A&M University Collaborative Program.

REFERENCES

Abdel-Wahhab, M.A., Hasan, A.M., Aly, S.E., and Mahrous, K.F. (2005) Adsorption of sterigmatocystin by montmorillonite and inhibition of its genotoxicity in the Nile tilapia fish (Oreachromis nilaticus). *Mutation Research-Genetic Toxicology and Environmental Mutagenesis*, **582**, 20−27.

Afriyie-Gyawu, E., Ankrah, N.A., Huebner, H.J., Ofosuhene, M., Kumi, J., Johnson, N.M., Tang, L., Xu, L., Jolly, P.E., Ellis, W.O., Ofori-Adjei, D., Williams, J.H., Wang, J.S., and Phillips, T.D. (2008a) NovaSil clay intervention in Ghanaians at high risk for aflatoxicosis. I. Study design and clinical outcomes. *Food Additives & Contaminants, Part A: Chemistry, Analysis, Control, Exposure & Risk Assessment*, **25**, 76−87.

Afriyie-Gyawu, E., Wang, Z., Ankrah, N.A., Xu, L., Johnson, N.M., Tang, L., Guan, H., Huebner, H.J., Jolly, P.E., Ellis, W.O., Taylor, R., Brattin, B., Ofori-Adjei, D., Williams, J.H., Wang, J.S., and Phillips, T.D. (2008b) NovaSil clay does not affect the concentrations of vitamins A and E and nutrient minerals in serum samples from Ghanaians at high risk for aflatoxicosis. *Food Additives & Contaminants, Part A: Chemistry, Analysis, Control, Exposure & Risk Assessment*, **25**, 872−884.

Bailey, C.A., Latimer, G.W., Barr, A.C., Wigle, W.L., Haq, A.U., Balthrop, J.E., and Kubena, L.F. (2006) Efficacy of montmorillonite clay (NovaSil PLUS) for protecting full-term broilers from aflatoxicosis. *Journal of Applied Poultry Research*, **15**, 198−206.

Billes, F., Móricz, A.M., Tyihák, E., and Mikosch, H. (2006) Simulated vibrational spectra of aflatoxins and their demethylated products and the estimation of the energies of the demethylation reactions. *Spectrochimica Acta Part A − Molecular and Biomolecular Spectroscopy*, **64**, 600−622.

Chaturvedi, V.B. and Singh, K.S. (2002) Detoxification of aflatoxin by adsorbents. *Indian Journal of Animal Sciences*, **72**, 924−927.

Chaturvedi, V.B., Singh, K.S., and Agnihotri, A.K. (2002) In vitro aflatoxin adsorption capacity of some indigenous aflatoxin adsorbents. *Indian Journal of Animal Sciences*, **72**, 257−260.

Colvin, B.M., Sangster, L.T., Haydon, K.D., Beaver, R.W., and Wilson, D.M. (1989) Effect of a high affinity aluminosilicate sorbent on prevention of aflatoxicosis in growing pigs. *Veterinary and Human Toxicology*, **31**, 46−48.

Deng, Y. and Szczerba, M. (2011) Computational evaluation of bonding between aflatoxin B_1 and smectite. *Applied Clay Science*, **54**, 26−33.

Deng, Y., Barrientos Velazquez, A.L., Billes, F., and Dixon, J.B. (2010) Bonding mechanisms between aflatoxin B_1 and smectite. *Applied Clay Science*, **50**, 92−98.

Desheng, Q., Fan, L., Yanhu, Y., and Niya, Z. (2005) Adsorption of aflatoxin B_1 on montmorillonite. *Poultry Science*, **84**, 959−961.

Dixon, J.B., Kannewischer, I., Tenorio Arvide, M.G., and Barrientos Velazquez, A.L. (2008) Aflatoxin sequestration in animal feeds by quality-labeled smectite clays: an introductory plan. *Applied Clay Science*, **40**, 201−208.

Egawa, T., Watanabe, H., Fujimura, T., Ishida, Y., Yamato, M., Masui, D., Shimada, T., Tachibana, H., Yoshida, H., Inoue, H., and Takagi, S. (2011) Novel methodology to control the adsorption structure of cationic porphyrins on the clay surface using the "size-matching rule". *Langmuir*, **27**, 10722−10729.

Ellis, R.W., Clements, M., Tibbetts, A., and Winfree, R. (2000) Reduction of the bioavailability of 20 μg/kg aflatoxin in trout feed containing clay. *Aquaculture*, **183**, 179−188.

Grant, P.G. and Phillips, T.D. (1998) Isothermal adsorption of aflatoxin B_1 on HSCAS clay. *Journal of Agricultural and Food Chemistry*, **46**, 599−605.

Grant, P.G., Lemke, S.L., Dwyer, M.R., and Phillips, T.D. (1998) Modified Langmuir equation for S-shaped and multisite isotherm. *Langmuir*, **14**, 4292−4299.

Gu, B.G., Schmitt, J., Chen, Z., Llang, L., and McCarthy, J.F. (1994) Adsorption and desorption of natural organic matter on iron oxide: Mechanisms and models. *Environmental Science & Technology*, **28**, 38−46.

Ishida, Y., Masui, D., Tachibana, H., Inoue, H., Shimada, T., and Takagi, S. (2012) Controlling the microadsorption structure of porphyrin dye assembly on clay surfaces using the "size-matching rule" for constructing an efficient energy transfer system. *ACS Applied Materials & Interfaces*, **4**, 811−816.

Kannewischer, I., Tenorio, A.M.G., White, G.N., and Dixon, J.B. (2006) Smectite clays as adsorbents of aflatoxin B_1: Initial steps. *Clay Science*, **12**(Supplement 2), 199−204.

Kubena, L.F., Harvey, R.B., Huff, W.E., and Corrier, D.E. (1990) Efficacy of a hydrated sodium calcium aluminosilicate to reduce the toxicity of aflatoxin and T-2 toxin. *Poultry Science*, **69**, 1078−1086.

Kunze, G.W. and Dixon, J.B. (1986) Pretreatment for mineralogy analysis. Pp. 91−100 in: *Methods of Soil Analysis Part 1: Physical and Mineralogical Methods,* 2nd edition (A. Klute, editor). Soil Science Society of America, Inc., Madison, Wisconsin, USA.

Laird, D.A., Barriuso, E., Dowdy, R.H., and Koskinen, W.C. (1992) Adsorption of atrazine on smectites. *Soil Science Society of America Journal*, **56**, 62−67.

Lindemann, M.D., Blodgett, D.J., Kornegay, E.T., and Schurig, G.G. (1993) Potential ameliorators of aflatoxicosis in weanling growing swine. *Journal of Animal Science*, **71**, 171−178.

Liu, C., Li, H., Johnston, C.T., Boyd, S.A., and Teppen, B.J. (2012) Relating clay structural factors to dioxin adsorption by smectites: molecular dynamics simulations. *Soil Science Society of America Journal*, **76**, 110−120.

Magnoli, A.P., Cabaglieri, L.R., Magnoli, C.E., Monge, J.C., Miazzo, R.D., Peralta, M.F., Salvano, M.A., Rosa, C.A.R., Dalcero, A.M., and Chiacchiera, S.M. (2008a) Bentonite performance on broiler chickens fed with diets containing natural levels of aflatoxin B_1. *Revista Brasileira De Medicina Veterinaria*, **30**, 55−60.

Magnoli, A.P., Tallone, L., Rosa, C.A.R., Dalcero, A.M., Chiacchiera, S.M., and Torres Sanchez, R.M. (2008b) Commercial bentonites as detoxifier of broiler feed contaminated with aflatoxin. *Applied Clay Science*, **40**, 63−71.

Márquez, R.N. and Hernandez, I.T.D. (1995) Aflatoxin adsorbent capacity of two Mexican aluminosilicates in experimentally contaminated chick diets. *Food Additives and Contaminants*, **1995**, 431−433.

Masimango, N., Remacle, J., and Ramaut, J.L. (1978) The role of adsorption in the elimination of aflatoxin B_1 from contaminated media. *European Journal of Applied Microbiology and Biotechnology*, **6**, 101−105.

Masimango, N., Remacle, J., and Ramaut, J. (1979) Elimination of aflatoxin B_1 from contaminated media by swollen clays. *Annales de la Nutrition et de l'Alimentation*, **33**, 137−1−47.

Mulder, I., Tenorio Arvide, M.G., White, G.N., and Dixon, J.B. (2008) Smectite clay sequestration of aflatoxin B_1: Mineral dispersivity and morphology. *Clays and Clay Minerals*, **56**, 559−571.

Pereira, T.R., Laird, D.A., Thompson, M.L., Johnston, C.T., Teppen, B.J., Li, H., and Boyd, S.A. (2008) Role of smectite

quasicrystal dynamics in adsorption of dinitrophenol. *Soil Science Society of America Journal*, **72**, 347–354.

Phillips, T.D., Kubena, L.F., Harvey, R.B., Taylor, D.R., and Heidelbaugh, N.D. (1988) Hydrated sodium calcium aluminosilicate: A high affinity sorbent for aflatoxin. *Poultry Science*, **67**, 243–247.

Phillips, T.D., Sarr, A.B., and Grant, P.G. (1995) Selective chemisorption and detoxification of aflatoxins by phyllosilicate clay. *Natural Toxins*, **3**, 204–213.

Phillips, T.D., Lemke, S.L., and Grant, P.G. (2002) Characterization of clay-based enterosorbents for the prevention of aflatoxicosis. Pp. 157–171 in: *Mycotoxins and Food Safety*. *Advances in Experimental Medicine and Biology*, vol. **504**. Kluwer Academic Publishers, Dordrecht, The Netherlands/Plenum Publishers, New York.

Phillips, T.D., Afriyie-Gyawu, E., Williams, J., Huebner, H., Ankrah, N.A., Ofori-Adjei, D., Jolly, P., Johnson, N., Taylor, J., Marroquin-Cardona, A., Xu, L., Tang, L., and Wang, J.S. (2008) Reducing human exposure to aflatoxin through the use of clay: A review. *Food Additives & Contaminants, Part A: Chemistry, Analysis, Control, Exposure & Risk Assessment*, **25**, 134–145.

Qi, D., Liu, F., Yu, Y., He, W., and Zhang, N. (2004) Detoxification of aflatoxin B1 contamination with montmorillonite. *Zhongguo Liangyou Xuebao*, **19**, 71–75.

Schulthess, C.P. and Dey, D.K. (1996) Estimation of Langmuir constants using linear and nonlinear least squares regression analyses. *Soil Science Society of America Journal*, **60**, 433–442.

Sheng, G., Johnston, C.T., Teppen, B.J., and Boyd, S.A. (2002) Adsorption of dinitrophenol herbicides from water by montmorillonites. *Clays and Clay Minerals*, **50**, 25–34.

Smith, E.E., Phillips, T.D., Ellis, J.A., Harvey, R.B., Kubena, L.F., Thompson, J., and Newton, G. (1994) Dietary hydrated sodium calcium aluminosilicate reduction of aflatoxin M1 residue in dairy goat milk and effects on milk production and components. *Journal of Animal Science*, **72**, 677–82.

Su, C.-C. and Shen, Y.-H. (2009) Adsorption of poly(ethylene oxide) on smectite. Effect of layer charge. *Journal of Colloid and Interface Science*, **332**, 11–15.

Takagi, S., Eguchi, M., Tryk, D.A., and Inoue, H. (2006) Light-harvesting energy transfer and subsequent electron transfer of cationic porphyrin complexes on clay surfaces. *Langmuir*, **22**, 1406–1408.

Takagi, S., Konno, S., Ishida, Y., Ceklovsky, A., Masui, D., Shimada, T., Tachibana, H., and Inoue, H. (2010) A unique "flattening effect" of clay on the photochemical properties of metalloporphyrins. *Clay Science*, **14**, 235–239.

Takagi, S., Aratake, Y., Konno, S., Masui, D., Shimada, T., Tachibana, H., and Inoue, H. (2011) Effects of porphyrin structure on the complex formation behavior with clay. *Microporous and Mesoporous Materials*, **141**, 38–42.

Takahashi-Ando, N., Kimura, M., Kakeya, H., Osada, H., and Yamaguchi, I. (2002) A novel lactonohydrolase responsible for the detoxification of zearalenone: enzyme purification and gene cloning. *Biochemical Journal*, **365**, 1–6.

Tenorio, A.M.G., Mulder, I., and Dixon, J.B. (2008) Smectite clay adsorption of aflatoxin vs. octahedral composition as indicated by FTIR. *Clays and Clay Minerals*, **56**, 571–578.

van Soest, T.C. and Peerdeman, A.F. (1970) The crystal structures of aflatoxin B_1. I. The structure of the chloroform solvate of aflatoxin B_1 and the absolute configuration of aflatoxin B_1. *Acta Crystallographica*, **B26**, 1940–1947.

Viani, A., Gualtieri, A.F., and Artioli, G. (2002) The nature of disorder in montmorillonite by simulation of X-ray powder patterns. *American Mineralogist*, **87**, 966–975.

Wang, P., Afriyie-Gyawu, E., Tang, Y., Johnson, N.M., Xu, L., Tang, L., Huebner, H.J., Ankrah, N.A., Ofori-Adjei, D., Ellis, W., Jolly, P.E., Williams, J.H., Wang, J.S., and Phillips, T.D. (2008) NovaSil clay intervention in Ghanaians at high risk for aflatoxicosis: II. Reduction in biomarkers of aflatoxin exposure in blood and urine. *Food Additives & Contaminants, Part A: Chemistry, Analysis, Control, Exposure & Risk Assessment*, **25**, 622–634.

(*Received 7 March 2012; revised 7 July 2012; Ms. 659; AE: R. Mikutta*)